External locating of moving targets for 3D IMRT using parallax method

Jian-Ning Han*, Peng Yang, Lu Zhang

School of Information and Communication Engineering, North University of China, 3 Xue Yuan Road, Taiyuan, China

Abstract

Due to the complexity of intensity modulated radiotherapy, it is difficult to meet the current situation of treatments which require real time locating of moving target. In this paper, we propose a new method based on parallax method using external label to locate the moving target. A column test-piece is used to simulate the human body structure for data analysis. A defect model for human body target is implanted inside the test-piece, which is the moving target. Based on the parallax method, the depth of the defect can be obtained by using the two images captured before and after the test-piece moves a short distance. The possible errors which affect the test results are analysed. The effects of errors can be reduced by adjusting the system parameters. The results show that the parallax method is a simple but efficient approach, which can be used for locating moving target in intensity modulated radiotherapy.

Keywords: Intensity modulated radiotherapy, Moving target location, Parallax method, Three-dimensional location, External Label

1 Introduction

Nowadays, intensity modulated radiotherapy has been able to realize the appropriate radiotherapy for a static target according to its height [1]. However, while the target moves during the process of radiotherapy, the blurring effects and the interaction between fringes of image will occur [2]. Therefore, it is difficult to arrange an appropriate dose arrangement for the moving target due to the dynamic state of human body structure, for instance, the tumor target in the human organs such as chest, stomach or prostate of a patient.

Recently, there are some studies on the target real time locating method. For instance, accurate real time dynamic information of the target can be obtained by implanting the signal responder unit inside the target. However, it also increases the complexity. More studies focus on the metal label's image inside the target to detect real time location. Until now, on the latest conventional accelerator, only 1KV ray source and one image device are installed vertically on the treatment ray bundle. Although the stereoscopic image location of the target can be achieved by using MV ray and KV ray treatment in some situation, the shadow of the label on EPID within the ray scope of the intensity modulated radiotherapy will often be sheltered from the MLC, which will have an effect on the location. However, the contrast ratio of MV image is far less than KV image, which makes it difficult to identify inner label in practice [3].

More recently, additional dimensional imaging equipment are used to process real time moving target location in some medical centres. For example, IRIS system (integrated radiotherapy imaging system) [8, 9] which can be installed on the accelerator's rack and rotates with the rack or RTRT system (Real-time tumor-tracking system). But these equipment not only expensive but also bring overdose imaging for patients during treatment. Considering these reasons, lots of studies try to use one direction LV X-ray imaging to achieve the real-time location for moving targets. Because the method is simple to apply and no need to use extra equipment, the dose for imaging of can be reduced. In this paper, we present a new three-dimensional locating approach for moving targets by using external label, which combines the features of moving targets with the theory of parallax method. A column test-piece with inner defects is used to simulate the human body targets. This real time locating method for the moving target can be used to get information for gating radiotherapy or tracking radiotherapy [4, 5].

2 System model design for radiation examination

2.1 IMAGING SYSTEM

Our method uses a column test-piece to represent the organization of human body. The internal defects of cylinder simulate he target area of the human body. The cylinder movement represents the human organ motion, The single direction X-ray system is shown Figure 1. The medical X-ray system is shown in Figure 2, Figure 3 shows the defects in cylinder which are very similar to human target area [6].

Corresponding author e-mail: hanjn46@nuc.edu.cn
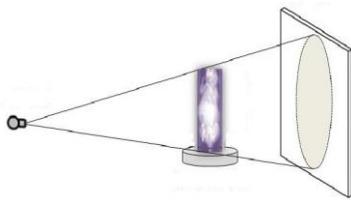
FIGURE 1 Medical Single direction X-ray system
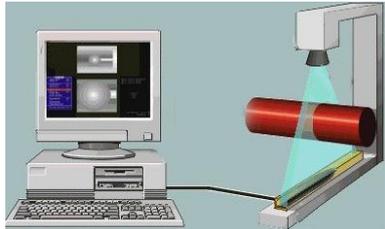
FIGURE 2 The Simulation of medical X-ray system
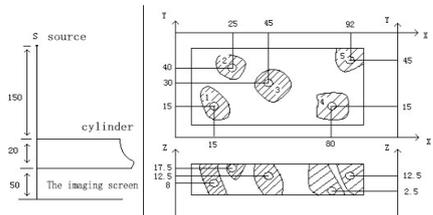
FIGURE 3 The cylinder with internal defects

2.2 MATHEMATICAL MODEL

We use the parallax method for defect locating. It is based on the straight propagation characteristics of radiation and the theory of triangle line similarity. A point (an object) at different locations of the two planes has been used to determine the spatial position. The schematic diagram is shown in Figure 4 [7].
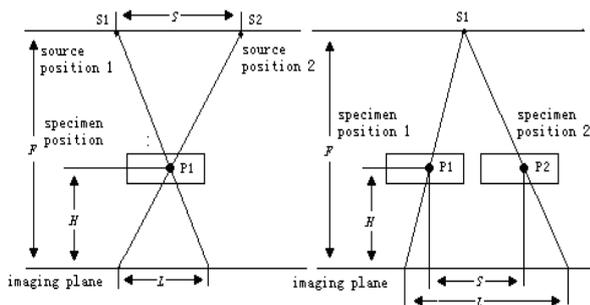
FIGURE 4 Parallax method principle diagrams

The left part of Figure 4 shows the locating method that the ray source moves. Ray source moves from S1 position to S2 position, the corresponding image point P1 has a displacement of L [8].

Using the triangle similarity relation, we can get:

$$H = LF/(S + L),$$ (1)

wherein:

H-the distance from defects to imaging plane;

F-the distance from ray source to imaging plane;

S- displacements between ray source exposure;

L-parallax, that is the displacement of defect projection.

Among them, F, S, L can be directly measured or indirectly measured by other methods and the defect depth can be obtained the quantity into Equation (1).

The right part of Figure 2 shows the locating method that specimen moves and ray source is motionless. Using the geometry relations:

$$H = F*(1 - S/L),$$ (2)

wherein:

H, F are consistent with an earlier statement;

S-displacements between ray source exposure；

L-parallax, that is the displacement of defect projection;

The final result of two methods are the same. Either method can be used for locating moving targets.

3 Defects in three-dimensional location

The schemes of defect location can be divided into direct measurement method, single labelled point method and multiple labelled point method. These three methods are based on the principle of parallax. Among them, direct measurement method is the simplest one. It applies the parallax principle model directly and obtains the defect under one coordinate system's absolute coordinate. Because the coordinate is not direct-viewing, so the method is impractical. Single labelled point method is quite easy and practical, it based on a marked point which is put on the specimen surface as a reference point. Finally we obtain the defect point coordinates relative to the reference point. It is intuitive and accurate, and it is the method we will adopt. The principle of double labelled point method and the single labelled point method are same, but they are complicated. Here we will mainly introduce the single labelled point method [9].

As is shown in Figure 4, putting a reference point on the surface of an object, we can use the equation to get the three-dimensional coordinates of M:

$$\begin{cases} X_M = L_M x_M / S \\ Y_M = L_M y_M / S \\ Z_M = F*(1 - S/L_M) \end{cases},$$ (3)

$$\begin{cases} X = L_D x_D / S - L_M x_M / S \\ Y = L_D y_D / S - L_M y_M / S \\ Z = F*(1 - S/L_D) - F*(1 - S/L_M) \end{cases}.$$ (4)

After simplification, we have:

$$\begin{cases} X = (L_D x_D - L_M x_M)/S \\ Y = (L_D y_D - L_M y_M)/S \\ Z = FS*(1/L_M - 1/L_D) \end{cases}.$$ (5)

From the above equations, we know that we need to determine the origin of coordinate in the process of measuring the x_D, y_D, x_M, y_M. But the process of subtraction can greatly eliminate common errors, and the coordinates got by this method are intuitive and easy to understand. We can use the laser illuminates along the rays to imaging screen and the screen image point of the laser can be used as the origin of the coordinate system [10].
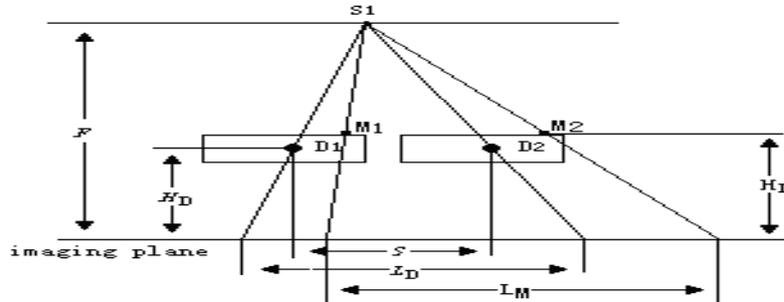
FIGURE 5. Single point external labelled defect location plans

4 Error analysis for defect location

4.1 THE UNCERTAINTY ESTIMATION OF INDIRECT MEASUREMENT

Because the three-dimensional coordinates of defect (x, y, z) are indirect measurement result, which cannot be measured directly, we firstly introduce the uncertainty estimation of indirect measurement.

If indirect measurement value N is the function of independent direct values of $x, y, z : N = f(x, y, z)$. And x, y, z contain errors, so N must contain errors. When the error is small, according to the Taylor series expansion, the uncertainty of each direct measurement result can be obtained by the uncertainty of indirect measurement result, which is called synthesis of uncertainty. There are two basic uncertainty synthesis methods [11-12].

If $\sigma_x, \sigma_y, \sigma_z$ are standard deviation of x, y, z, σ_N, the standard deviation of N is given by the following equation:

$$\sigma_N = \sqrt{(\frac{\partial f}{\partial x}\partial x)^2 + (\frac{\partial f}{\partial y}\partial y)^2 + (\frac{\partial f}{\partial z}\partial z)^2} \quad . \tag{6}$$

It turns out that no matter what probability distribution x, y, z is, this equation is tenable and this method is called the square root synthesis of standard deviation.

If e_x, e_y, e_z are error range of x, y, z, we can obtain e_N (the error range of N) through the arithmetic synthesis method:

$$e_N = \left|\frac{\partial f}{\partial x}\right| e_x + \left|\frac{\partial f}{\partial y}\right| e_y + \left|\frac{\partial f}{\partial z}\right| e_z \tag{7}$$

It is more reliable using arithmetic synthesis method when we estimate error range, although it often tends to be conservative [13].

4.2 UNCERTAINTY ANALYSIS OF THE PARALLAX METHOD

In direct measurement method, the standard deviation of X_D, Y_D, Z_D are $\sigma_{X_D}, \sigma_{Y_D}, \sigma_{Z_D}$ list as follows:

$$\sigma_{X_D} = \sqrt{(\frac{\partial f}{\partial L_D}\partial L_D)^2 + (\frac{\partial f}{\partial x_D}\partial x_D)^2 + (\frac{\partial f}{\partial S}\partial S)^2}$$

$$\sigma_{Y_D} = \sqrt{(\frac{\partial f}{\partial L_D}\partial L_D)^2 + (\frac{\partial f}{\partial y_D}\partial y_D)^2 + (\frac{\partial f}{\partial S}\partial S)^2} \tag{8}$$

$$\sigma_{Z_D} = \sqrt{(\frac{\partial f}{\partial F}\partial F)^2 + (\frac{\partial f}{\partial S}\partial S)^2 + (\frac{\partial f}{\partial L_D}\partial L_D)^2}$$

and can be simplified as:

$$\sigma_{X_D} = \sqrt{(\frac{x_D}{S}\partial L_D)^2 + (\frac{L_D}{S}\partial x_D)^2 + (\frac{L_D x_D}{S^2}\partial S)^2}$$

$$\sigma_{Y_D} = \sqrt{(\frac{x_D}{S}\partial L_D)^2 + (\frac{L_D}{S}\partial y_D)^2 + (\frac{L_D x_D}{S^2}\partial S)^2} \tag{9}$$

$$\sigma_{Z_D} = \sqrt{((1 - S/L_D)\partial F)^2 + (\frac{F}{L_D}\partial S)^2 + (\frac{FS}{L_D^2}\partial L_D)^2}$$

error range:

$$e_{X_D} = \left|\frac{\partial f}{\partial L_D}\right|e_{L_D} + \left|\frac{\partial f}{\partial x_D}\right|e_{x_D} + \left|\frac{\partial f}{\partial S}\right|e_S$$

$$e_{Y_D} = \left|\frac{\partial f}{\partial L_D}\right|e_{L_D} + \left|\frac{\partial f}{\partial y_D}\right|e_{y_D} + \left|\frac{\partial f}{\partial S}\right|e_S \qquad (10)$$

$$e_{Z_D} = \left|\frac{\partial f}{\partial F}\right|e_F + \left|\frac{\partial f}{\partial S}\right|e_S + \left|\frac{\partial f}{\partial L_D}\right|e_{L_D}$$

and finally we have:

$$e_{X_D} = \left|\frac{x_D}{S}\right|e_{L_D} + \left|\frac{L_D}{S}\right|e_{x_D} + \left|\frac{L_D x_D}{S^2}\right|e_S$$

$$e_{Y_D} = \left|\frac{y_D}{S}\right|e_{L_D} + \left|\frac{L_D}{S}\right|e_{y_D} + \left|\frac{L_D y_D}{S^2}\right|e_S \qquad . \qquad (11)$$

$$e_{Z_D} = |1 - S/L_D|e_F + \left|\frac{F}{L_D}\right|e_S + \left|\frac{FS}{L_D^2}\right|e_{L_D}$$

From the above two equations, we can see that the error of x_D is introduced by L_D, x_D, S. Its error transfer functions can be shown as $\frac{x_D}{S}, \frac{L_D}{S}, \frac{L_D x_D}{X^2}$. In the process of measuring X_D, we properly identify the distance from ray source to the object and the distance from object to the imagining screen. Make sure the two values were comparable, and there is no big value in three errors transfer coefficient. Thus, in the process of measuring X_D, each component's influence on the measurement results are within the normal range. In a similar way, the error of Y_D is introduced by L_D, x_D, S. Its error transfer coefficient can be shown as $\frac{y_D}{S}, \frac{L_D}{S}, \frac{L_D y_D}{X^2}$, and there is also no big component, so the process of measuring Y_D can also be normal. The error of Z_D is introduced by F, S, L_D, its error transfer coefficient can be shown as, $1 - S/L_D$, $F/L_D, FS/L_D^2$. Due to the companionability of S and L_D, the first component is not seriously amplified. Between the two components, the value of F is larger than the other parameters value. Therefore, the measured results are mainly influenced by S, L_D.

From the above analysis, we can see that the existence of error propagation makes measurement affected by the error of the measurement components. Here we should pay attention to Z_D, namely the deriving of defect depth which is greatly affected by S and L_D. If the value of $\frac{F}{L_D}$ and $\frac{FS}{L_D^2}$ are lager, we should reduce the two rations appropriately in order to reduce the error. But under the influence of geometric sharpness of imaging systems, the values of $\frac{F}{L_D}, \frac{FS}{L_D^2}$ must be not too small. So we can only try to improve the accuracy of S and L_D. S is the moving distance of test specimen, and is influenced by mechanical platform. The precision of the platform we used is 0.005mm. If F is about 1000mm, L_D is about 30mm, then $\left|\frac{F}{L_D}\right|e_S$ is 0.16mm [14-15].

5 Analysis of experimental images and data

As shown in Figure 3, the distance from point to the workpiece is 150mm, the distance from the workpiece to the imaging screen is 50mm, the thickness of workpiece itself is 20mm, so we can know that F is 220mm. The simulation of workpiece is 100x50x20mm. There are five point defects. We will locate the point defects with the parallax method, and make a comparison with the original coordinates.

Errors are added in simulations in order to simulate the real situation. In Figure 6, the left image is for the first location image, the middle one is after moving the point source, and Figure 6(c) is the composite image by matching two images. The ray source moves along the X-axis, so there is only the parallax between the composite images along the x-axis. Therefore, the 3 dimensional coordinates of the defect can be calculated according to the parallax images and the mathematical model.
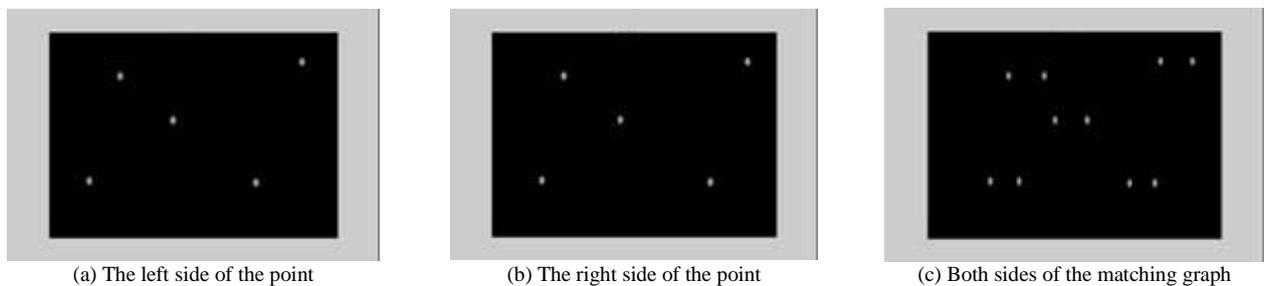
(a) The left side of the point (b) The right side of the point (c) Both sides of the matching graph
FIGURE 6 The simulation of defect projecting

Table 1 shows the comparison between the two coordinators when the error of point source movement is 0.2mm, image movement measurement error has 2 pixels, and measuring focal distance error is 0.2mm.

TABLE 1 The correlation table of seeking coordinate and original coordinate

former	X(mm)	Y(mm)	Z(mm)	calculate	X(mm)	Y(mm)	Z(mm)
1	15	15	8	1	15.102	15.102	8.00087
2	25	40	17.5	2	25.105	40.00084	17.501
3	45	30	12.5	3	45.120	30.00064	12.5009
4	80	15	2.5	4	80.152	15.00034	2.50082
5	92	45	12.5	5	92.153	45.00097	12.5009

In the experiment, the major errors are the relative parameters errors in the testing and the systematic error in application of the system. The latter is mainly the error caused by the radio source.

Figure 7 shows the relationship between H and k=S/L when ΔF is fixed as 0.2mm, 0.5mm, 0.8mm, and 1.0mm respectively. ΔH can be expressed as: $\Delta H = \Delta F/(k+1)$. It can be seen that ΔH is greatly reduced as k increases.
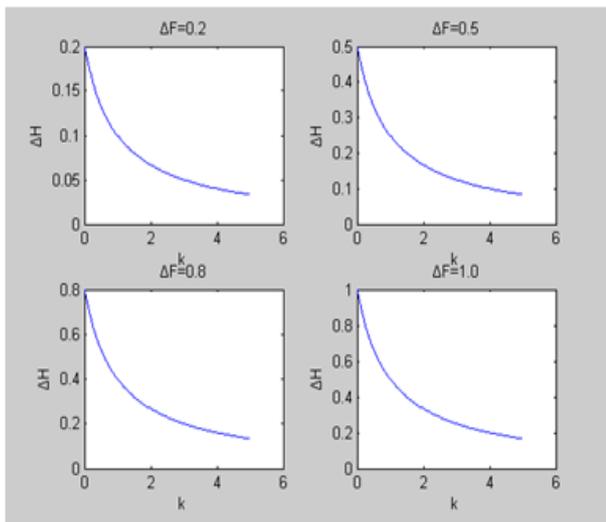
FIGURE 7 The relationship between k and ΔH when fixing ΔF

Figure 8 shows the relationship of k and ΔH when S=0.2mm, 0.5mm, 0.8mm, 1.0mm. $\Delta H = k \cdot F \cdot \Delta S/S/(k+1)/(k+1+\Delta S/L) \approx \Delta H = k \cdot F \cdot \Delta S/S /(k+1)^2$. It can be seen that the influence of ΔS on H is affected by

the value of k. So k can be appropriately increased to reduce the influence of ΔS on the final measurement of H. Compared with the former two testing errors, the error caused by ΔL is pixel level, which can be neglected.
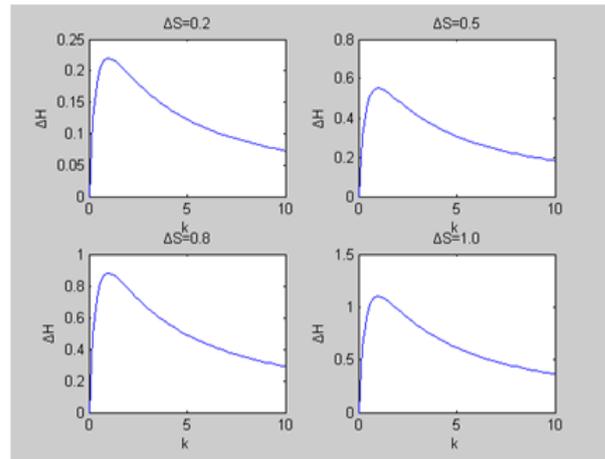
FIGURE 8 The relationship between k and ΔH when fixing ΔS

Table 2 is the coordinates when ΔF=0.5mm and ΔS=0.5mm. It can be observed that the influence of ΔF is smaller than the one of ΔS. Considering the practical testing precision can reach 0.2mm, the practical error will be smaller than that shown in the table.

TABLE 2 ΔF and ΔS on the result of measurement

insertΔF	X(mm)	Y(mm)	Z(mm)	insertΔS	X(mm)	Y(mm)	Z(mm)
1	14.904	14.904	8.132	1	15.139	15.139	7.776
2	24.898	39.869	17.654	2	25.176	40.222	17.236
3	44.858	29.905	12.642	3	45.227	30.185	12.256
4	79.762	14.955	2.620	4	80.190	15.035	2.304
5	91.709	44.858	12.642	5	92.260	45.1279	12.256

6 Conclusions

In conclusion, the parallax method is used in the external label for locating moving targets in 3D IMRT. The theoretical model based on parallax method theory is discussed and errors of parameters in measurement are analysed in detail. The images of the external labelled points at different positions are acquired in the experiment with moving ray source and fixed the workpiece. The error of defect location is about 0.2mm when the precision of testing workbench is 0.005mm,

and the distance from the ray source to image plane is 1000mm. This accuracy of measurement can meet the needs for 3D IMRT applications. Comparing with the traditional radiograph examination method, the external label method based on parallax theory is more flexible, and precise to be applied in practice.

Acknowledgements

References

[1] Bertuzzi A, Bruni C, Papa F 2013 Optimal solution for a cancer radiotherapy problem *Journal of Mathematical Biology* **66**(1-2) 311-49

[2] Van Herk M 2004 Errors and margins in radiotherapy *Seminars in Radiation Oncology* **14**(1) 52-64

[3] Gilliom J, Monahan T 2012 *Supervision: an introduction to the Surveillance Society* University of Chicago Press: Chicago

[4] Wiersma R D, Mao W, Xing L 2008 Combined kV and MV imaging for real-time tracking of implanted fiducial markersa *Medical Physics* **35**(4) 1191-8

[5] DeKay S H 2012 Interpersonal communication in the workplace: A largely unexplored region *Business Communication Quarterly* **75**(4) 449-50

[6] Kieffer J C, Krol A, Jiang Z 2002 Future of laser-based X-ray sources for medical imaging *Applied Physics B* **74**(1) 75-81

[7] Banerjee K, Dunn W L 2007 On X-ray back-scattering to detect hidden cracks in multi-layer structures *Applied Radiation and Isotopes* **65**(2) 176-7

[8] Liu C, Lee J, Jing J 2010 Motions of hard x-ray sources during an asymmetric eruption *The Astrophysical Journal Letters* **721**(2) 193-8

[9] Silverman D 2013 *Doing qualitative research: A practical handbook* SAGE Publications Limited: London.

[10] Liao T W 2009 Improving the accuracy of computer-aided radiographic weld inspection by feature selection *NDT& E International* **42**(4) 229-39

[11] FU Li-qin, HAN Yan 2008 Study on Stereo Matching Technique for Digital Radiography Images *Journal of Image and Graphics* **13**(12) 2363-7 (In Chinese)

[12] da Silva R R, Mery D 2007 State-of-the-Art of weld seam inspection by radiographic testing: part i–image processing *E-Journal of Nondestructive Testing and Ultrasonics* **12**(4) 1-9

[13] CHEN Ming, MA Yuezhou, CHEN Guang 2007 Weld defects detection for X-ray linear array real-time imaging *Transactions China Welding Institution* **28**(6) 81-4 *(in Chinese)*

[14] Sim L M, Tan T C, Mon A A 2009 X-ray absorption-based technique to measure the thickness of multilayered structures *NDT & International* **42**(4) 291-6

[15] Dahai R, Zheng Y, Changku, S 2000 Automatic Analysing System of X-ray Real-time Radiography for Welds *Transactions China Welding Institution* **21**(1) 60-3 *(in Chinese)*

Authors

Jian-ning Han, born in December, 1980, China County, Shanxi Province, P.R. China

Current position, grades: Lecturer of School of Information and Communication Engineering, North University of China, China.
University studies: B.Sc. in Electronic information engineering from North University of China in China. M.Sc. from North University of China in China.
Scientific interest: Acoustic signal processing, Graphics processing
Publications: more than 7 papers published in various journals.
Experience: teaching experience of 11 years, 5 scientific research projects.

Peng Yang, born in July, 1988, China County, Shanxi Province, P.R. China

Current position, grades: student of School of Information and Communication Engineering, North University of China, China.
University studies: B.Sc. in Electronic information engineering from North University of China in China. M.Sc. from North University of China in China.
Scientific interest: Acoustic signal processing.
Experience: researching experience of 2 years, 1 scientific research project.

Lu Zhang, born in July, 1988.07, China County, Shanxi Province, P.R. China

Current position, grades: student of School of Information and Communication Engineering, North University of China, China.
University studies: B.Sc. in Electronic information engineering from North University of China in China. M.Sc. from North University of China in China.
Scientific interest: Acoustic signal processing,
Experience: researching experience of 1 year, 1 scientific research projects.

Nature Phenomena and Innovative Engineering